Hierarchical Self-Organization of ABC Terpolymer Constituted of a Long Polyelectrolyte End-Capped by Different Hydrophobic Blocks

Ilias Katsampas and Constantinos Tsitsilianis*

Department of Chemical Engineering, University of Patras, 26504 Patras, Greece, and Institute of Chemical Engineering and High-Temperature Chemical Processes, ICE/HT-FORTH, P.O.Box 1414, 26504 Patras, Greece

Received August 23, 2004; Revised Manuscript Received November 25, 2004

ABSTRACT: The self-organization of a mono hydrophilic ABC terpolymer, which is constituted of a central long polyelectrolyte end-capped by two different hydrophobic short blocks (i.e., polystyrene-*b*-poly(acrylic acid)-*b*-poly(*n*-butyl methacrylate), PS−PAA−PnBMA), was examined in aqueous salt-free dilute solutions by static and dynamic light scattering, scanning electron microscopy, and rheology. The neutralized PS−PAA−PnBMA terpolymer is self-organized hierarchically from flowerlike micelles to dendronlike micellar aggregates and eventually to a three-dimensional physical network. The rheological properties of the resulting physical gel were also investigated and discussed.

Introduction

ABC triblock terpolymers comprise a relatively new and interesting macromolecular architecture, as they consist of three chemically different components, each one conferring to the polymer one different function. Attention was payed first on the synthesis and the properties of ABC copolymers in the bulk state. Provided that sufficient incompatibility exists between the blocks, this type of copolymers can form three microphases in the bulk,[1] leading to novel morphologies which depend on the volume fractions and the interaction parameters of the copolymer components.[2−7]

In recent years an increasing number of works have appeared concerning the behavior of the ABC terpolymers in solution.[8−20] In this case, the solvent is the fourth component, which plays a very important role in the self-organization of the terpolymer. The interaction parameters among the different component increase with respect to the bulk state, increasing therefore the diversity of the system and leading to novel macromolecular self-assemblies.

Micelles of complex structures such as ABC core−shell−corona structures (onion type)[12] shell cross-linked micelles,[19] core cross-linked Janus micelles,[18] crew cut micelles,[16] and heteroarm starlike micelles[17] have appeared recently. Three are the key factors that determine their structure in solution: topology of the different blocks, selectivity of the solvent, and specific interactions among the unlike segments.

In the case where the solvent is water, even more interesting and fascinating properties have appeared. If at least one of the components responses to changes of the aqueous environment such as pH, ionic strength, and temperature, then we are led to the so-called stimuli-responsive polymers with potential applications of great technological importance in biomedicine, cosmetics, coatings, etc.

Concerning the number of the hydrophilic blocks, the ABC terpolymers can be distinguished to mono,[15] double,[12] or even triple[19] hydrophilic terpolymers. In the first case, the species that have been studied so far are those that the hydrophilic block is located in the outer (A or C) position.

In this paper, the aqueous solution properties of a highly asymmetric mono hydrophilic ABC terpolymer with the hydrophilic part located in the middle position and behaving as a polyelectrolyte will be presented. As will be shown, the specific topology and the ionic nature of the hydrophilic part offer new possibilities of self-assembly. The terpolymer under investigation, termed also as "heterotelechelic polyelectrolyte", is a fully neutralized long poly(acrylic acid) (PAA) end-capped by polystyrene (PS) and poly(*n*-butyl methacrylate) (PnBMA) short blocks which exhibit different glass transition temperatures. The synthesis and preliminary rheological properties have been reported recently.[20] Herein we study the hierarchical self-assembly of this terpolymer as concentration increases by using static and dynamic light scattering, rheology, and scanning electron microscopy.

Experimental Section

Synthesis. The polymer sample (PS−PAA−PnBMA) was synthesized by anionic polymerization with sequential addition of the monomers and selective hydrolysis of the middle block. Details of the synthetic procedure were previously reported.[20]

The characterization of the ABC copolymer and its AB precursor was carried out by several methods such as size exclusion chromatography (SEC), ^{1}H NMR, static light scattering, and titration. The characterization data are presented in Table 1.

Light Scattering. Static light scattering (SLS) experiments were performed at 25 °C by means of a spectrogoniometer, model SEM RD (Sematech, France), with vertically polarized incident light of wavelength $\lambda = 633$ nm supplied by a He−Ne laser. The required specific refractive index increment dn/dc values were measured by a Chromatic KMX-16 differential refractometer operating at 633 nm.

The data of SLS were analyzed according to the Zimm method (eq 1)

$$Kc/(I - I_0) = 1/M_w + 2A_2c + ... \quad (1)$$

where I is intensity of light scattering from solution relative to that from benzene, I_0 is the corresponding quantity of the solvent, c is the concentration (in g/mL), M_w is the mass-average molar mass of the solute, A_2 is the second virial

* Corresponding author. E-mail ct@chemeng.upatras.gr.

10.1021/ma048275c CCC: $30.25
Published on Web 01/20/2005

Table 1. Molecular Characteristics of AB and ABC Copolymers

polymer	M_w/M_n	M_w(L−S)	PS	PtBA[a]	PnBMA
PS−PtBA (AB)	1.1	111 672	35 units	844 units	
PS−PtBA−PnBMA (ABC)	1.16	112 950	35 units	844 units	9 units

After Hydrolysis

polymer	hydrolysis deg (%)	$M_{w\,(calculated)}$	PS	PAA	PtBA	PnBMA
PS−PAA	98	65 343	35 units	827 units	17 units	
PS−PAA−PnBMA	98	66 621	35 units	827 units	17 units	9 units

[a] Poly(*tert*-butyl acrylate).

coefficient, and K is the appropriate optical constant, which includes the specific refractive index.

Intensity−time correlation functions $g_2(t)$ of the polarized light scattering were measured at $\theta = 90°$ at 25 °C with a full multiple tau digital correlator (ALV-5000/FAST) with 280 channels. The excitation light source was an argon ion laser (Spectra Physics 2020) operating at 488 nm, with a stabilized power of 30 mW. The incident beam was polarized vertically with respect to the scattering plane using a Glan polarizer. The scattered light from the sample was collected through a Glan-Thomson polarizer (Halle, Berlin) with an extinction coefficient better than 10^{-7}.

The correlation functions from DLS where analyzed by the constrained regularized CONTIN method to obtain distributions of decay times (Γ). The decay rate distributions gave distributions of apparent diffusion coefficient, $D_{app} = \Gamma/q^2$ ($q = (4\pi n/\lambda)\sin(\theta/2)$, n is the refractive index of the solvent), and hence of apparent hydrodynamic radius via Stokes−Einstein equation:

$$R_{h,app} = K_B T/(6\pi\eta D_{app}) \quad (2)$$

where K_B is the Boltzmann constant and η is the viscosity of the solvent at temperature T.

Rheology. Steady-state shear rheological measurements were carried out on a controlled stress rheometer, Rheometric Schientific (SR-200). The shear stress was varied between 0.06 and 500 Pa to obtain shear rates in the range 0.001 and 1000 s^{-1}. Cone and plate (diameter 40 mm, cone angle 0.04 rad, gap 0.053 mm) and Couette geometry (with cup 50 mm diameter, bob 48 mm diameter) were used for the high- and low-viscosity samples, respectively. All the measurements were performed at 25 °C. A solvent trap was used to minimize changes in concentrations due to water evaporation. The sample concentration was varied between 0.05 and 2 wt %. The zero-shear viscosity (η_0) was obtained from Step Stress Creep (creep compliance, $J_{(t)}$, vs time) test. A steady-state creep compliance J^0 is defined by extrapolation at the limiting slope ($t = 0$). The slope is the inverse zero shear viscosity according to the following equation:

$$J_{(t)} = J^0 + \frac{t}{\eta_0} \quad (3)$$

For dynamic measurements, the stress values were chosen to perform the experiments in the linear viscoelastic regime. For this purpose, a preliminary study was made at constant angular frequency $\omega = 1$ Hz, and the linear viscoelastic region was determined for each measurement, i.e., the limiting stress under which rheological parameters (G', G'') remained constant.

Sample Preparation. For the rheology measurements the solutions were directly prepared to the final desired concentration. A proper amount of polymer (acid form) was weighted in a screw-capped vial. First an equivalent amount of 0.1 N NαOH was added to neutralize the PAA units and then water (Millipore Milli-Q) to the final volume. The samples were stirred and heated for 48 h at 100 °C. This is the time required to attain equilibrium. They were centrifuged several times for short periods during the heating procedure for better solution mixing and removing of bubbles. After equilibrium was attained the samples were allowed to cool to room temperature and were weighted. The concentrations were corrected to take into account possible loss of water (less than 1%) during the heating procedure. Good reproducibility in the rheological properties was found after that treatment. The samples where checked after the thermal treatment by ^{1}H NMR showing that the PnBMA end blocks remained intact.

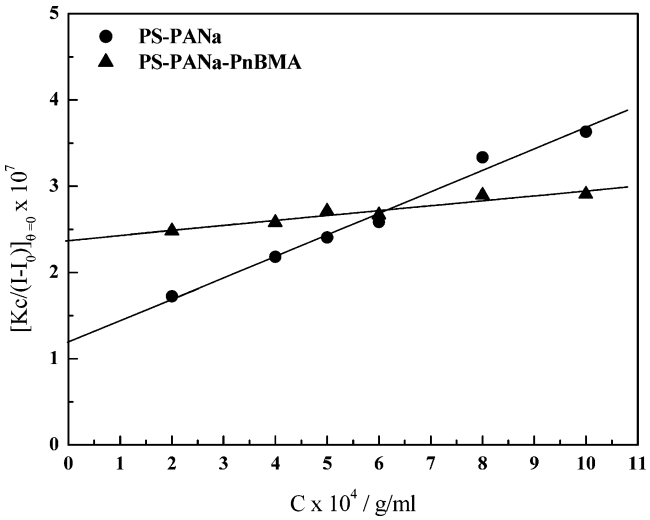

Figure 1. $Kc/(I - I_0)_{\theta=0}$ vs concentration for the AB and ABC copolymers.

For the light scattering measurements a mother solution with a concentration of 0.1 wt % was prepared by the same procedure. Several concentrations ranging from 0.1 to 0.0125 wt % were prepared by dilution. The solutions for the light scattering experiments were carefully filtered through 0.5 μm Millipore filters.

Scanning Electron Microscopy (SEM). The morphology of aggregates was observed by LEO SUPRA 35VP scanning electron microscopy. The samples were prepared by spin-coating of dilute polymer solutions on mica substrates and covered with gold.

Results and Discussion

Micellar Nanostructures at Low Concentrations. Static and dynamic light scattering experiments were first used to study the self-organization of the ABC copolymer in dilute aqueous solutions. For the shake of comparison the behavior of the AB precursor was also examined.

Values of $Kc/(I - I_0)$ extrapolated to zero angle ($\theta = 0$) were plotted as a function of concentration for both ABC and AB copolymers in Figure 1. From the extrapolated value at zero concentration, the apparent molecular weight of aggregates and therefore the aggregation number ($N_{agg} = M_{w,micelle}/M_{w,unimer}$) could be estimated. As expected, the determined molecular weights were found much higher than those of the copolymers revealing the formation of micelles with N_{agg} 102 and 50 for the AB and ABC, respectively. Although the light scattering measurements have been performed in salt-

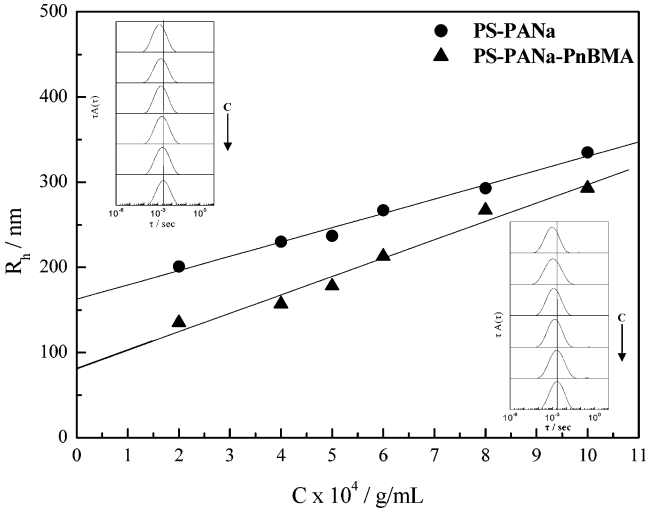

Figure 2. Concentration dependence of the apparent hydrodynamic radius for the AB and ABC copolymers. The insets show the relaxation time distribution for each concentration: upper left, AB; lower right, ABC.

free aqueous solutions, the linear concentration dependence in Figure 1 seems to be unaffected from the polyelectrolyte effect. Also, the angular dependence of the scattering data does not show any anomalous curvature which could be arisen from interparticle interference. In a previous work, Eisenberg et al.[21] determined N_{agg} for the $Ps_{23}-PANa_{300}$ in very low salt concentration ($C_s = 0.05$ M) to be 87. Using the data in other salt concentrations from the same work, the extrapolated value in salt-free solution is estimated to be 85. It is known that N_{agg} depends mainly on the insoluble block length N_B and decreases smoothly with the soluble block length N_A. According to the mean-field theory proposed by Leibler et al.[22] $N_{agg} \sim N_B^{0.6}$. For $N_B = 35$ (present polymer) the estimated N_{agg} value should be 109, which is in very good agreement with the experimental value found herein. Therefore, the apparent molecular weights estimated in the present work seem to be reasonable. Surprisingly the value of the ABC terpolymer was considerably lower, although it bears higher number of hydrophobic units with respect to the AB precursor.

Dynamic light scattering experiments were performed for both copolymers, over the same polymer concentration range, to get the hydrodynamic dimensions of the micelles. The autocorrelation functions, $g_2(t)$, were analyzed using CONTIN analysis in terms of a continuous distribution of relaxation times which are shown in the insets of Figure 2. In all cases monomodal distribution functions were obtained. The average relaxation time was determined from the peak of the relaxations curves. The apparent hydrodynamic radius was calculated through (eq 2) and plotted vs concentration. Extrapolation of the data to zero polymer concentration (essentially equivalent to zero micelle concentration) gave the values of the hydrodynamic radius R_h of the micelles. The R_h of the AB (162 nm) is double than that of ABC (81 nm). Again, the dynamic light scattering results clearly show that the size of the micelles formed from the ABC terpolymer was considerably lower than that of the AB precursor it originated from.

To verify the light scattering results and to explore the morphology of the micelles, scanning electron microscopy has been employed. SEM images obtained on

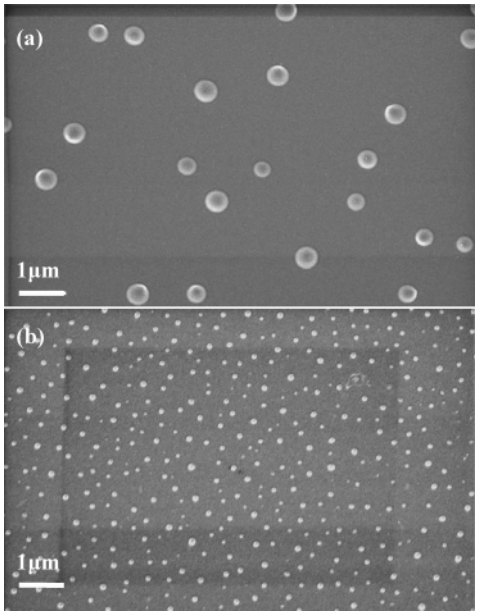

Figure 3. SEM images of AB (a) and ABC (b) copolymer micelles onto mica surface from $c = 0.01$ wt %.

mica substrate by spin-coating of 0.01 wt % polymer solutions are illustrated in Figure 3. Small, good shaped spherical particles for the ABC copolymer and significantly larger for the AB precursor can be observed corroborating the light scattering findings that ABC terpolymers form much smaller micelles with respect to the AB diblocks revealing the strong influence of the macromolecular architecture.

The question that has to be answered is, "what is the internal structure of the ABC micelles"? As it is known from previous studies, the AB amphiphilic polyelectrolytes with asymmetric long hydrophilic chain form starlike micelles with a core−shell structure where the corona chains adopt a stretched conformation due to the repulsive electrostatic interactions of the charges located along the chain.[21,23] Indeed, in the case of the AB precursor the hydrodynamic radius is about the 77% of the contour length of the fully stretched PAA chains ($844 \times 0.25 = 211$ nm).

In the case of the ABC, the PAA middle block is now end-capped at both ends by hydrophobic blocks. Therefore, the conformation of the hydrophilic chains is influenced by two antagonistic factors: the hydrophobic attractive interactions between PS and PnBMA end blocks that tend to form looping chains and the repulsive electrostatic interactions along the chain that tend to stretch them. Therefore, there is interplay between the energy gain due to the association of the chain ends (stickers) and the entropy loss due to the extension of the chains as well as the translational entropy of the counterions. This antagonism may lead to two possible internal structures of the micelles with spherical shape: flowerlike micelles constituted of a hydrophobic core surrounded by corona with looping chains or finite size clusters which are in fact microgels with many hydrophobic cross-links interconnected by stretched chains as proposed by theoretical considerations recently.[24]

Our findings suggest that in the range of concentrations studied flowerlike micelles seem to be formed. The fact that the aggregation number and the hydrodynamic radius of the ABC micelles are about the half of those of the AB precursor corroborate this assumption. The

number of single hydrophilic chains in stretched conformation (AB) in the protected corona is equivalent to half number of looping chains (ABC) that eventually seems to stabilize the micellar structure. In both cases the number of the hydrophobic end blocks is the same. It should be noted that back-folding of the charged polyelectrolyte chains is not prevented, since the persistent length is much shorter than the contour length of the PAA block.

The core of the micelles is composed from PS and PnBMA short polymeric chains, and the question that emerges is whether they are mixed or phase separated. Assuming that we have a dry core, the product of the Flory interaction parameter χ_{AC} with the number of the repeating units N ($N_A + N_C$) was calculated to 2.3 ,[25] which is lower than the theoretical predictions for the critical point of demixing of homopolymer blend given by $\chi N = 4$,[26] showing that in the present case cores with mixed chains are likely to be formed.

Another specific feature of the ABC structure with respect to that of the ABA[27,28] is that the outer hydrophobic blocks differ significantly in their length and more importantly in their T_g's (the T_g for PnBMA is much lower than that of PS). The T_g of the PnBMA end blocks is lower than room temperature, inducing higher segmental mobility in the hydrophobic cores. Consequently, the C block can act as a "surfactant" tail that is able to exchange between the aggregates and the aqueous environment, facilitating therefore the intermicellar association as will be shown below.

Association of Micelles into Dendronlike Cluster. At concentrations above 0.1 wt % the micelles start to be associated in a second level of hierarchy. In Figure 4 SEM images of associated micelles, deposited on mica substrate by weak centrifugal forces, are illustrated. As can be seen in the inset of Figure 4b at even lower concentrations (c = 0.05 wt %), some micelles already form intermicellar associates. At higher concentrations bigger micellar aggregates with irregular shape are formed which tend to be further accumulated into dendron like micellar clusters (Figure 4c). On the contrary, such clusters were not observed from the AB copolymer at the same concentration (Fi4a).

In Figure 5 SEM images obtained from a thin film cast from a dilute ABC micellar solution (0.15 wt %) is illustrated. Close-packed dendrons like micellar structures have been obtained. It is interesting to note that the images on this film are reminiscent of the spherulites in semicrystalline polymers. Indeed, a radial growth of the dentronlike structures of the micellar clusters truncated by impingement can be observed.

The driving force for such an association process is the possibility of the different hydrophobic end blocks of the macromolecular chain to be located in two different micellar hydrophobic cores. In other words, at higher concentrations conformational transitions from looping to extending PAA chains occur, the latter performing as bridges between adjacent micelles. This loop to bridge transition has also been observed in nonionic associative ABA amphiphilic block copolymers, which form transient networks above a certain concentration.[29] The difference in the present case is that additional forces arisen from the electrostatic repulsive interactions along the hydrophilic middle chain favor stretched chain conformations, which in turn favor loop to bridge transitions. In the present case these transitions seem to occur at much lower concentrations and

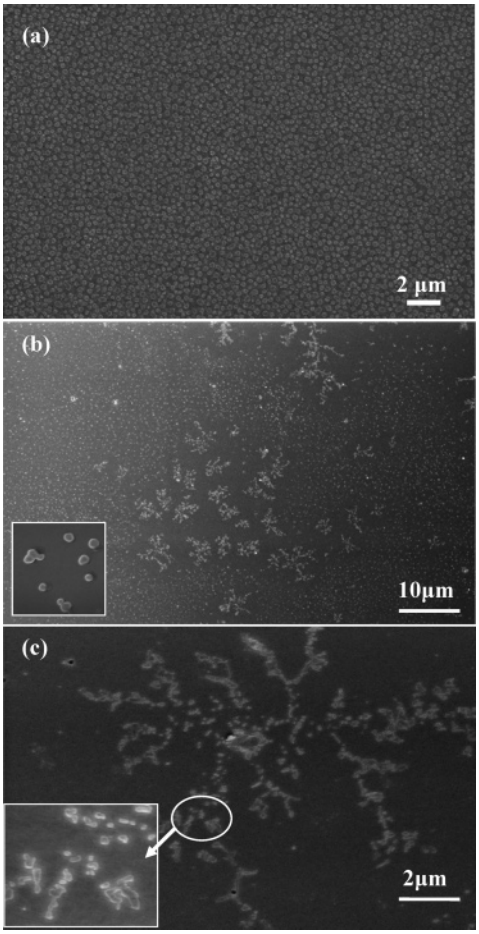

Figure 4. SEM images of AB (a) spherical micelles and ABC (b, c) dendronlike morphologies at c = 0.1 wt % onto mica surface at different magnification. In the inset of (b) c = 0.05 wt %.

to a higher extent with respect to nonionic telechelic associative polymers, decreasing therefore the gel concentration and increasing the plateau modulus, as will be discussed below.

It should be mentioned here that association of polyelectrolyte starlike micelles constituted of poly(ethylethylene)−poly(styrenesulfonic acid) diblock amphiphilic copolymers is also possible through a different association mechanism. As has been reported, micellar strings forming cross-links, loops, and toroids, and eventually networks with fractal structure can be formed by increasing the ionic strength of the solution. In this case, micelle association occurs through weak attractive electrostatic interactions arisen from transient fluctuations in the periphery of the micellar corona.[30]

Three-Dimensional Transient Network. At slightly higher concentrations, i.e., C_p = 0.15 wt %, the solution becomes very viscous, revealing the onset of the formation of a highly structured fluid. In this case, it is reasonable to accept that extending loop to bridge transitions occur which rapidly leads to the formation of a three-dimensional transient network, as we have reported previously.[20] Figure 6 illustrates the morphology of a 3D dry physical gel obtained by freeze-drying of 1 wt % aqueous solution on mica substrate. An irregular highly microporous material has been formed.

To study further the higher concentration regime, steady state and oscillatory rheological experiments

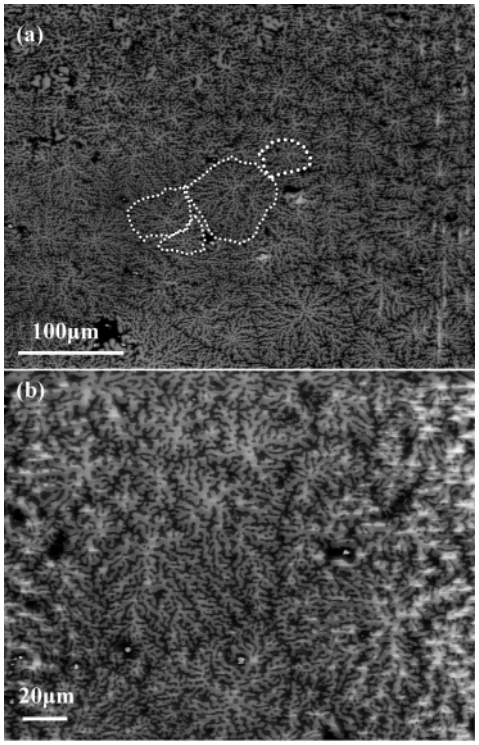

Figure 5. SEM images of ABC copolymer thin film on to mica surface after solvent evaporation at two different magnifications. The close dot lines at the upper figure assign the limits of individual morphologies.

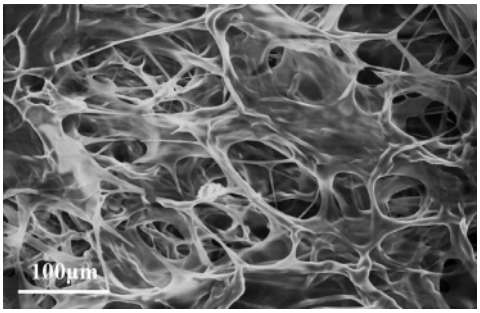

Figure 6. SEM image of ABC physical hydro gel after freeze-drying.

were carried out. Recent rheological experiments[20,28] in associative telechelic polyelectolytes have shown complicated viscosity profiles, i.e., yield stress followed by three shear thinning regimes. To further explore this behavior, steady-state shear flow measurements and creep test were carried out for several concentrations. Figure 7 shows a typical variation of the steady-state viscosity of an ABC aqueous solution ($c = 1$ wt %) as a function of the shear stress. As can be seen, the viscosity profile eventually is richer with respect to that reported previously.[20] By creep measurements a Newtonian plateau was observed at low shear stresses, which corresponds to a very low shear rate regime (below 10^{-4} s^{-1}) that could not be reached by ordinary stress sweep test. The Newtonian plateau is followed by a strong shear-thinning effect. Indeed, above a certain stress a dramatic drop of the viscosity, about 3 orders of magnitude, is evidenced. This stress was attributed to a yield stress behavior, since the Newtonian plateau had not been determined. In fact, this stress is an apparent yield stress above which a breakage of the infinite physical three-dimensional network into finite-size clusters (microgels) is likely to occur. Similar experimental results with pronounced shear thinning behavior have also been observed for multisticker associative polymers[31] and nonionic telechelics.[32] In the latter case this effect is of lower magnitude.

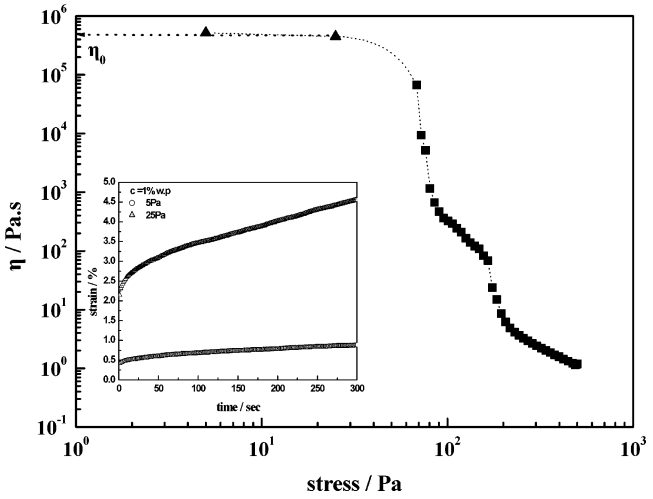

Figure 7. Steady-state shear viscosity of the ABC aqueous polymer solution as a function of applied stress. The triangle symbols extracted from creep experiments (inset figure), and the square symbols extracted from stress ramp tests.

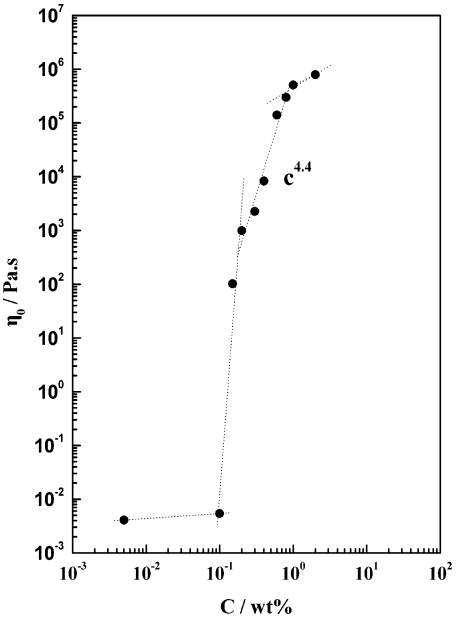

Figure 8. Effect of concentration on zero shear viscosity (η_0) of the ABC terpolymer.

At higher shear stresses, a smooth shear thinning can be seen followed by a second sharp decrease of viscosity (about 1 order of magnitude) in a narrow shear stress range. This discontinuity has been attributed to a further disruption of the large clusters to smaller fragments.[20]

The above findings allowed us to determine the zero shear viscosity of the solutions, which is plotted as a function of polymer concentration in Figure 8. Several concentration regimes can be distinguished. In the region below $c = 0.1$ wt % the polymer solutions behave as Newtonian fluids, which is consistent with the existence of micellar nanoparticles as discussed previously. Above $c = 0.1$ wt % and in a very narrow concentration range ($0.1 < c < 0.2$ wt %), the viscosity

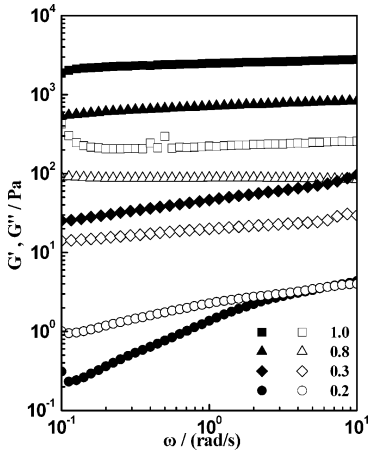

Figure 9. G' (filled symbols) and G'' (open symbols) as a function of frequency for the ABC terpolymer at various concentrations in wt %.

jump about 5 orders of magnitude in consistent with a percolation process. This is really a unique behavior which has not been observed for other associative polymers so far. The concentration of 0.1 wt % is identified as the gelation concentration (c_g) above which an infinite transient network has started to be built by interconnection of the flowerlike micelles into dendron-like micellar clusters through loop to bridge transitions as revealed by SEM imaging.

At higher concentration and in the range $0.2 < c < 1.0$ wt %, the zero viscosity continues to increase with a power law $\eta_0 \sim c^{4.4}$, reaching a value that is 8 orders of magnitude higher than that in the gel threshold. In this regime further association of the finite size micellar clusters occurs, leading to the formation of an infinite three-dimensional physical network. Finally, at the highest concentrations the values of the zero viscosity tends to level off.

Interesting information on the internal structure of the network could be gained by oscillatory rheological measurements in the linear viscoelastic regime. Characteristic frequency spectra of various solutions above c_g, showing the elastic (G') and viscous (G'') modulus as a function of frequency, are depicted in Figure 9. At concentrations above $c = 0.3$ wt % the elastic modulus G' exceeds the viscous modulus G'' in the whole frequency range investigated. At $c = 1.0$ wt %, G' is 1 order of magnitude higher than G'', and both are nearly independent of frequency showing that the system behaves as an elastic soft solid. Such behavior is characteristic of a physical gel consisting of strong physical bonds as it has been discussed recently.[29] In a first approximation G' could be considered as the plateau modulus, G_N^0, which is related to the number density of the elastically active chains (bridging chains) of the network, v, through the Green−Tobolsky theory on rubber elasticity (eq 4)[33]

$$G_N^0 = gvK_BT \tag{4}$$

where g is a correction factor usually taken as unity for systems with large junction functionality, K_B the Boltzmann constant, and T the absolute temperature.

Figure 10 shows the concentration dependence of G_N^0 and the reduced modulus G_N^0/nK_BT which reflects the fraction of bridging chains between the hydrophobic cores v/n (n denotes the number density of total chains in the solution) calculated through eq 5.

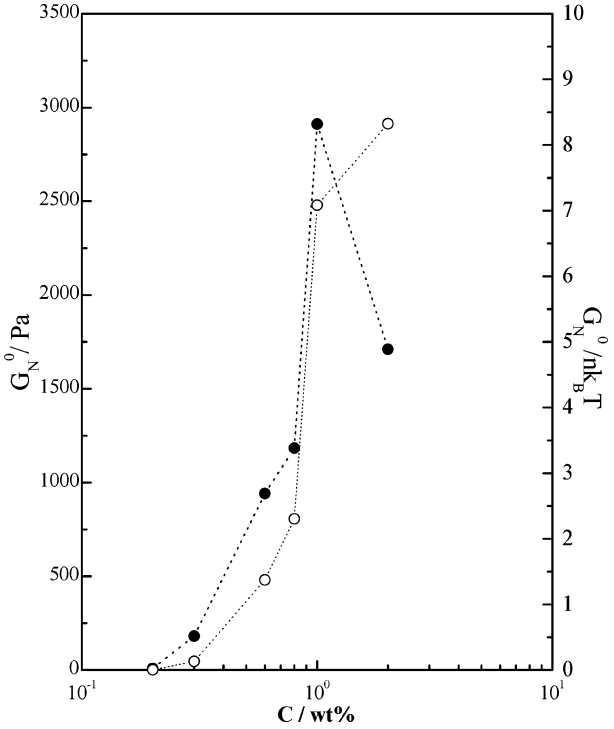

Figure 10. Concentration dependence of the plateau modulus (open symbols) and the fraction of bridging chains (filled symbols).

$$\frac{v}{n} = \frac{G_N^0}{nK_BT} \tag{5}$$

As is demonstrated, G_N^0 increases monotonically with concentration, reflecting an increase of the number of the elastic chains arisen from loop to bridge transitions. However, better insight could be gained by plotting the concentration dependence of the reduced modulus (Figure 10). The magnitude of the fraction of bridging chains exceeds unity above $c = 0.3$ wt %, indicating an extra contribution to the plateau modulus, reaching a maximum at $c = 1.0$ wt % while decreasing at $c = 2.0$ wt %. Again, the v/n of 8 at 1.0 wt % is much higher than that found in nonionic telechelic associative polymers[34] and in accordance with that observed in the PS−PAA−PS system. This behavior was discussed in detail recently[29] and was attributed to the ionic character of the bridging chains. The repulsive electrostatic interactions, due to the presence of charges along the bridging chains, provoke a double effect. On one hand, it favors loop to bridge transitions increasing therefore the number density of the elastically active chains, and on the other hand, it imposes a stretched conformation of the bridging chains, contributing to excess values on the plateau modulus.[29]

At higher concentrations than 1 wt % although G_N^0 continuous to increase, the reduced plateau modulus decreases, and this should be ascribed to the fact that the bridging chains are less stretched due to screening effect arisen from the ionic strength enhancement.

Gelation Mechanism. In light of the present experimental findings, a gelation mechanism could be proposed as schematically represented in Figure 11. The association process is governed by the competition between the attractive hydrophobic interactions of the

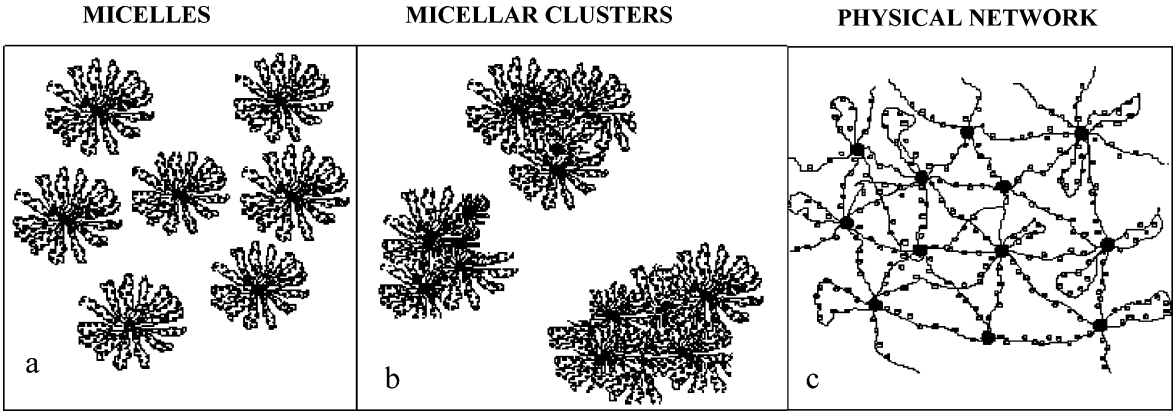

Figure 11. Schematic representation of the gelation mechanism of the PS−PANa−PnBMA/water system.

Table 2. Molecular Characteristics of AB and ABC Micellesin Dilute Aqueous Solutions

polymer	M_w	N_{agg}	R_H (nm)
PS−PANa	8 407 000	102	162
PS−PANa−PNBMA	4 211 000	50	81

sticky outer A and C blocks and the repulsive electrostatic interactions along the hydrophilic B middle block. At low concentrations, the hydrophobic interactions between the outer blocks overcome the repulsive interactions along the middle chain, leading to the formation of flowerlike micelles (Figure 11a). Above a certain concentration, the electrostatic interactions favor loop to bridge transitions and corroborated from the easier exchange of the C block; the micelles are associated into micellar clusters (Figure 11b). The number of these transitions increases rapidly leading to the formation of a 3D physical network (Figure 11c) with significant higher fraction of bridging chains with respect to the nonionic associative telechelic polymers.

Conclusions

The hierarchical self-organization of a mono hydrophilic ABC terpolymer constituted of a central long polyelectrolyte end-capped by two different hydrophobic short blocks, PS−PAA−PnBMA, has been studied in aqueous salt-free dilute solutions.

The association process is governed mainly by two antagonistic factors: the intramolecular hydrophobic attractive interactions between the end blocks and the repulsive electrostatic interactions along the chain. In the first level of association the hydrophobic interactions predominate and flowerlike spherical micelles with looping polyelectrolyte chains seem to be formed. Above a critical concentration the repulsive electrostatic interactions favor loop to bridge transitions, and in a second level of hierarchy, association of micelles occurs, leading to the development of dendronlike aggregates and eventually to a three-dimensional transient network.

One of the important consequences of the ABC architecture with respect to AB is its capability to form physical gels at very low concentrations with interesting rheological properties and therefore broader potential applications. A more detailed rheological investigation showed the following: The steady-state shear viscosity profile is more complex, characterized by a Newtonian plateau at very low shear rates, an apparent yield stress, and several shear thinning regimes. The gel concentration was determined at $c = 0.1$ wt %, which is even lower than that of PS−PAA−PS triblock copolymer.[27] The concentration dependence of the zero shear viscosity is also presented, characterized by a very abrupt viscosity increase, which tend to level of at 2 wt % polymer concentration.

Finally, the effect of the hydrophilic chain stretched conformation on the plateau modulus was also confirmed for the end-capped polyelectrolytes. The degree of stretching can be monitored by the external conditions like pH and ionic strength, which in turn will influence all the solution properties. Therefore, this ABC terpolymer belongs to the category of stimulus responsive associative polymers and further work is in progress to explore its behavior in different environments.

Acknowledgment. Helpful discussions and suggestions from Dr I. Iliopoulos are greatly appreciated. We also thank Dr. S. N. Yannopoulos and Dr. V. Dracopoulos for their assistance in the dynamic light scattering and scanning electron microscopy experiments, respectively. I.K. thanks the Institute of Chemical Engineering and High Temperature Chemical Processes for financial support.

References and Notes

(1) Leibler, L.; Fredrickson, G. H. *Chem. Br.* **1995**, 42.
(2) Lohse, D. J.; Hadjichristidis, N. *Curr. Opin. Colloid Interface Sci.* **1997**, *2*, 171.
(3) Kudose, I.; Kotaka, T. *Macromolecules* **1984**, *17*, 2325.
(4) Mogi, Y.; Mori, K.; Matsushita, Y.; Noda, I. *Macromolecules* **1992**, *25*, 5412.
(5) Auschra, C.; Stadler, R. *Macromolecules* **1993**, *26*, 2171.
(6) Gido, S. P.; Schwark, D. W.; Thomas, E. L.; Gonçalves, M. C. *Macromolecules* **1993**, *26*, 2636.
(7) Lazzari, M.; Lòpez-Quintela, M. A. *Adv. Mater.* **2003**, *15*, 1583.
(8) Patrickios, C. S.; Hertler, W. R.; Abbott, N. L.; Hatton, T. A. *Macromolecules* **1994**, *27*, 930.
(9) Chen, W.-Y.; Alexandridis, P.; Su, C.-K.; Patrickios,; C. S.; Hertler, C. S.; Hatton, T. A. *Macromolecules* **1995**, *28*, 8604.
(10) Patrickios, C. S.; Forder, C.; Armes, S. P.; Billingham, N. C. *J. Polym. Sci., Part A: Polym. Chem.* **1997**, *35*, 1181.
(11) Patrickios, C. S.; Lowe, A. B.; Armes, S. P.; Billingham, N. C. *J. Polym. Sci., Part A: Polym. Chem.* **1998**, *36*, 617.
(12) Gohy, J.-F.; Willet, N.; Varshney, S.; Zhang, J.-X.; Jerome, R. *Angew. Chem.* **2001**, *113*, 3314.
(13) Triftaridou, A. I.; Vamvakaki, M.; Patrickios, C. S. *Polymer* **2002**, *43*, 2921.
(14) Giebeler, E.; Stadler, R. *Macromol. Chem. Phys.* **1997**, *198*, 3815.
(15) Kriz, J.; Masar, B.; Plestil, J.; Tuzar, Z.; Pospisil, H.; Doskocilova, D. *Macromolecules* **1998**, *31*, 41.
(16) (a) Yu, G.; Eisenberg, A. *Macromolecules* **1998**, *31*, 5546. (b) Liu, F.; Eisenberg, A. *J. Am. Chem. Soc.* **2003**, *125*, 15059.

(17) (a) Tsitsilianis, C.; Sfika, V. *Macromol. Rapid Commun.* **2001**, *22*, 647. (b) Sfika, V.; Tsitsilianis, C.; Kiriy, A.; Gorodyska, A.; Stamm, M. *Macromolecules* **2004**, *37*, 9551.
(18) Erhardt, R.; Zhang, M.; Boker, A.; Zettl, H.; Abetz, C.; Frederic, P.; Krausch, G.; Abetz, V.; Müller, A. *J. Am. Chem. Soc.* **2003**, *125*, 3260.
(19) Liu, S.; Weaver, J. V. M.; Tang, Y.; Billingham, N. C. Armes, S. P.; Tribe, K. *Macromolecules* **2002**, *35*, 6121.
(20) Tsitsilianis, C.; Katsampas, I.; Sfika, V. *Macromolecules* **2000**, *33*, 9054.
(21) Khougaz, K.; Astafieva, I.; Eisenberg, A. *Macromolecules* **1995**, *28*, 7135.
(22) Leibler, L.; Orland, H.; Wheeler, J. C. *J. Chem. Phys.* **1983**, *79*, 3550.
(23) Groenewegen, W.; Egelhaaf, S. U.; Lapp, A.; van der Maarel, J. R. C. *Macromolecules* **2000**, *33*, 3283.
(24) Potemkin, I. I.; Vasilevskaya, V. V.; Khokhlov, A. R. *J. Chem. Phys.* **1999**, *111*, 2809.
(25) Tsitsilianis, C. *Macromolecules* **1993**, *26*, 2977.
(26) de Gennes, P. G. *Scaling Concepts in Polymer Physics*; Cornel University Press: Ithaca, NY, 1979; Chapter 4.
(27) Winnik, M. A.; Yekta, A. *Curr. Opin. Colloid Interface Sci.* **1997**, *2*, 424.
(28) Tsitsilianis, C.; Iliopoulos, I.; Ducouret, G. *Macromolecules* **2000**, *33*, 2936.
(29) Tsitsilianis, C.; Iliopoulos, I. *Macromolecules* **2002**, *53*, 3662.
(30) Förster, S.; Abetz, V.; Müller, A. H. E. *Adv. Polym. Sci.* **2004**, *166*, 173.
(31) (a) Aubry, T.; Moan, M. *J. Rheol.* **1994**, *38*, 1681. (b) Kujawa, P.; Audibert-Hayet, A.; Selb, J.; Candau, F. *J. Polym. Sci., Part B: Polym. Phys.* **2004**, *42*, 1640.
(32) Tirtaatmadja, V.; Tam, K. C.; Jenkins, R. D. *Macromolecules* **1997**, *30*, 1426.
(33) Green, M. S.; Tobolsky, A. V. *J. Chem. Phys.* **1946**, *14*, 80.
(34) Pham, Q. T.; Russel, W. B.; Thibeault, J. C.; Lau, W. *Macromolecules* **1999**, *32*, 5139.

MA048275C